Procedia Manufacturing

Volume 5, 2016, Pages 1320–1336

44th Proceedings of the North American Manufacturing Research Institution of SME http://www.sme.org/namrc

Performance Enhancement of Cylindrical Grinding Process with a Portable Diagnostic System

R Vairamuthu[1] Brij M Bhushan[2] R Srikanth[1] and Ramesh Babu N[1*]

[1]*Department of Mechanical Engineering, Indian Institute of Technology, Madras.*

[2]*Graduate student, Massachusetts Institute of Technology, MA.*

r.vairamuthubds@gmail.com, nrbabu@iitm.ac.in

Abstract

Material removal processes are one among several manufacturing processes that necessitates the enhancement of their precision capability to cater the demanding needs of higher technological innovations. The performance of a material removal process depends on several factors like the precision of the machine tool, process parameters, process consumables and to a certain extent on the skill of the operator. This paper presents an approach to develop a diagnostic system that can enhance the performance of cylindrical grinding process by monitoring vital process signals like grinding power and infeed of axis. The developed diagnostic system comprises of a powercell and LVDT enabling the measurement of power drawn by wheel spindle along with the wheel infeed movement. Using the measured signals, the developed system is used to optimize the grinding cycle parameters in order to enhance the efficiency of the process. The effectiveness of the developed in-process portable diagnostic system is demonstrated with two case studies. The effect of dressing on the performance of the grinding process is explained in one of the case studies using the diagnostic tool. In another industrial case study, the application of diagnostic tool for selecting the grinding cycle and to determine the frequency of dressing is explained.

Keywords: Diagnostic system, Process monitoring, Power measurement, Optimization

1 Introduction

Grinding is a finishing process that controls the quality of components in terms of form, dimensions, finish and surface integrity. Apart from these outputs, it is important to determine the cycle-time and grinding costs for assessing the effectiveness of grinding. In brief, the entire grinding process can be viewed as an input-transformation-output system (Subramanian, 1992; Tönshoff, 2002) in which the inputs to the process include grinding machine tool, process parameters, work material properties, and tooling and the outputs of the process cover both technical and system outputs. Form, dimensions, finish

* Corresponding Author

 Selection and peer-review under responsibility of the Scientific Programme Committee of NAMRI/SME

doi:10.1016/j.promfg.2016.08.103

and integrity on part are the technical outputs while the productivity i.e. grinding cycle time and the cost of grinding are the system outputs. The performance of any grinding process can be enhanced by enhancing both technical and system outputs. In practice, the choice of grinding wheel and the conditions of grinding is made based on the work material and its geometry in order to realize the desired technical outputs (Subramanian, 1995).

The performance of a grinding process is highly influenced by the precision of grinder, the condition of wheel, the wheel and work interaction and process settings including the parameters chosen for dressing and grinding (Pawel and Jan, 1993). In grinding, the mechanics of material removal i.e. the interaction between abrasive grain and work-piece is quite complex due to the presence of several mechanisms such as cutting, plowing and rubbing between the grit and the work surface. In view of this complexity, it is often difficult to realize consistent results in grinding (Malkin and Guo, 2008; Subramanian, 1992). Moreover, the condition of grinding wheel i.e. the form and topography changes with every grinding cycle and is highly unpredictable. Hence, the performance of grinding process and optimal utilisation of grinding machine are mostly dependent on the skills of the operator. But, to realise consistent results of grinding, it is important to understand the behaviour of grinding process during grinding and then to select a suitable set of parameters for controlling the process. This demands for a system that can continuously monitor the grinding process and then suggest suitable set of measures for realizing consistent results in grinding.

Several attempts have been made to analyse the dynamic behaviour of grinding process by various process monitoring strategies. These strategies can be classified into continuous and periodic monitoring systems based on the nature of monitoring of parameters. Based on the nature of measurement of parameters, they can be divided into direct and indirect measurements (Byrne et al., 1995). Generally, the monitoring of grinding process is attempted by an indirect and continuous method of measurement. Tönshoff et al. (1992) summarized the different sensors employed for process monitoring along with different techniques of monitoring. These sensors essentially measure the force, temperature, vibration, acoustic emission and power that are in turn used to control the grinding process. Finally, their study has suggested the importance of integration of these sensors for closed loop of process monitoring, effective diagnosis of process and control of grinding process. Dornfeld and Cai (1984) have used Acoustic Emission (AE) sensor to monitor the loading of wheel in grinding process. Inasaki (1985) has proposed the use of AE sensor as a contact detector during approach of wheel and monitored the dressing process and then to control the surface finish achieved on the ground component. Pawel and Jan (1993) developed a multi-sensor fusion system including AE sensors, force and vibration sensors for monitoring of grinding wheel in cylindrical grinding and suggested the need to analyse the signals collected from different sensors to assess the process behavior. Karpuschewski et al. (2000) monitored the grinding and dressing process using power and AE sensors and used the signals measured to develop an artificial intelligence system for optimization of grinding parameters. But the application of AE sensors is highly affected by the coolant flow and bearing noise during grinding and prompted the need for tedious methods of post processing of signals to study the grinding process online and therefore limited its application to contact detection and wheel crash detection (Karpuschewski and Inasaki, 2005). Couey et al. (2005) used a non-contact displacement sensor embedded in aerostatic spindles to monitor the forces in cylindrical grinding. However, this method of monitoring of forces is found to be quite complex and expensive. 'Intelligent' grinding wheels mounted with thermocouples were used to measure the temperature directly at the wheel and work interaction zone. This direct and continuous measurement of temperature was used to correlate with the grinding process outcome to control the process performance (Brinksmeier et al., 2005). On the other hand, the measurement of temperature requires elaborate preparation of the wheel and is highly intrusive to the grinding process and has limited its capability to more academic research than industrial applications (Karpuschewski and Inasaki, 2005).

Oliveira et al. (2009) covered various challenges and opportunities that exist in grinding for arriving at industrially viable solutions. The effective monitoring of production cylindrical grinding process is still a great challenge in view of varying geometries of wheel employed for grinding of different

components. Finally, it summarized certain topics of industrial relevance that cover process reliability and diagnosis of grinding. Efforts are needed to select relevant process variables of grinding process that reflect the process dynamics and behavior.

From the above, it is clear that certain sensors like AE sensors, force and temperature sensors are found to be widely used for monitoring of grinding process and its outcomes. In practice, each of these sensors has its own drawbacks in effective monitoring of grinding process. On the contrary, the power drawn by electrical motor during grinding is much easier to measure and is also non-intrusive making it viable for continuous monitoring of process. It is seen that the choice of power as a potential measurand for grinding process monitoring is not fully explored (David and John 2003; Inasaki, 1999; Inasaki et al., 2000; Karpuschewski and Inasaki, 2005; Wei Tian, 2009; Xiao et al., 1992). Hence, it is reasonable to think of a compact, portable diagnostic system with power sensor for on-line monitoring of grinding process. When this sensor is combined with infeed displacement sensor, the combination of these sensors can analyse the performance of abrasive wheel in grinding.

This work covers the development of a diagnostic system for continuous monitoring of process with a view to suggest suitable measures to enhance the performance of a cylindrical grinding process. The diagnostic system consists of a process monitoring sensor systems, which comprises of a powercell and LVDT integrated with data acquisition system to monitor the grinding process continuously. The data collected is then analyzed to characterize the status of grinding process with varying wheel and work conditions including other parameters like dressing conditions, coolant flowrates etc. The integration of process monitoring, data analysis and corrective actuation (feedback) is used for design/redesign of cylindrical grinding process. Two case studies explain the effectiveness of the developed diagnostic system.

2 Structure of diagnostic system

Figure 1 gives a schematic of diagnostic tool developed for monitoring the performance of grinding process. It covers a) portable diagnostic tool with power and LVDT sensors and b) data extraction and analysis unit. In general, any process diagnostic system initially collects the data with a suitable set of sensors, and then analyses the collected data to indicate the status of the process. In case of grinding, the data collected from a set of sensors can be used to analyze the relevance of grinding cycle and also to analyze/estimate the performance of grinding process (Andrew et al., 2006). Therefore, the steps covered to diagnose a grinding process include: i) Process monitoring and data acquisition, ii) data analysis dealing with feature recognition and feature evaluation, and iii) inferences to suggest process enhancement strategies.

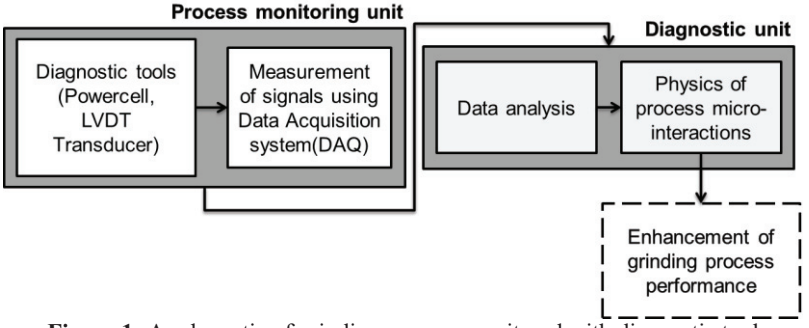

Figure 1: A schematic of grinding process monitored with diagnostic tool

2.1 Development of process-monitoring unit

Figure 2 shows a schematic of process monitoring in a cylindrical grinding machine during grinding. The process-monitoring unit comprises of a powercell, LVDT transducer and a data acquisition (DAQ) system. The powercell is a single/three phase AC and DC power measurement device with Hall-effect sensor for measuring the current while a bypass internal circuitry samples the voltage simultaneously. A vector multiplication of measured current and voltage value including the power factor and that enables the measurement of effective power drawn by the spindle motor during its operation. The powercell used in this work can measure power in the range of 5 HP– 150 HP with a resolution of 0.05 HP. The measured power is calibrated to a voltage output of 0-10V DC. The LVDT transducer is an integrated core, spring return plunger type displacement measurement device. This transducer can measure the displacement in the range of 0-10mm with a resolution of 1 micron and gives a calibrated voltage output of 0-10 V DC.

Both sensors were calibrated before measurements. Hall Effect sensor in the powercell was calibrated using a standard calibrated Hall device with adjustable flux density and an NI voltage DAQ. The LVDT was calibrated using a calibration check fixture i.e. a precision micrometer with LVDT mounting stand and an NI voltage DAQ. Both sensors are analog monitoring systems and a DAQ system is used to collect the signals from both sensors. The DAQ is primarily an analog to digital conversion system that enables the measured data to be stored in a computer. NI 9205 voltage DAQ is used to collect the sensor output from both power cell and LVDT transducer. The DAQ used can measure the output from 32 sensors simultaneously. Thus, the measured outputs from both the sensors are synchronized with time.

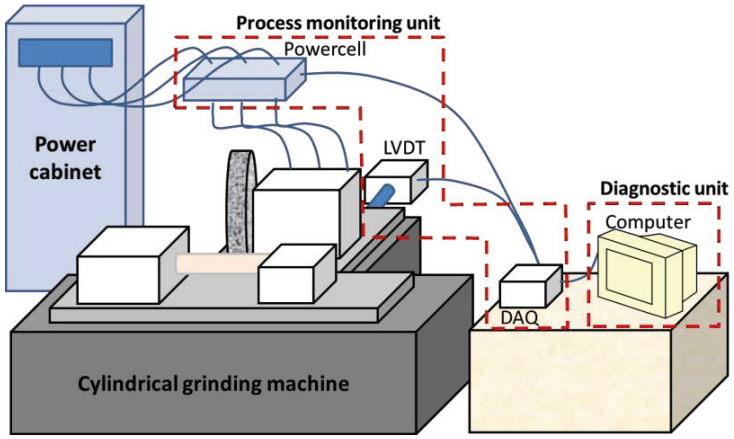

Figure 2: Schematic showing the arrangement of different sensors for monitoring the cylindrical grinding process

2.2 Measurement of spindle motor power

During grinding, the power drawn by wheel spindle motor is monitored with a powercell connected to the spindle motor input power line. Figure 3(a) shows the location of powercell in the electrical cabin of machine tool. The main power supply to the wheel spindle motor is routed through the powercell to measure the power drawn. Thus, this makes the powercell non-intrusive to the grinding zone.

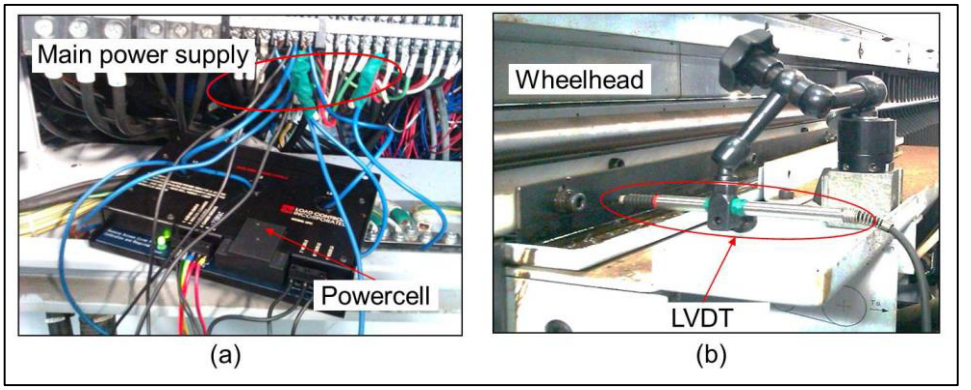

Figure 3: Mounting location of sensors in grinding machine tool (a) Powercell (b) LVDT

2.3 Measurement of infeed movement of wheelhead

The infeed of grinding wheel can be measured by measuring either the carriage slide movement or the movement of wheelhead with respect to some fixed reference. Figure 3(b) shows the mounting location of LVDT on the bed. It is held by a magnetic base articulated arm stand. The plunger of LVDT senses the feed movement of entire wheelhead during plunge grinding of component.

2.4 Data acquisition system

The output of powercell and LVDT are analog signals and are converted into digital form with data acquisition (DAQ) unit. Figure 4 shows the schematic of data acquisition. The analog signals from both sensors are captured and are digitized using a voltage DAQ and LabVIEW software. The signals are then stored in a computer for further analysis.

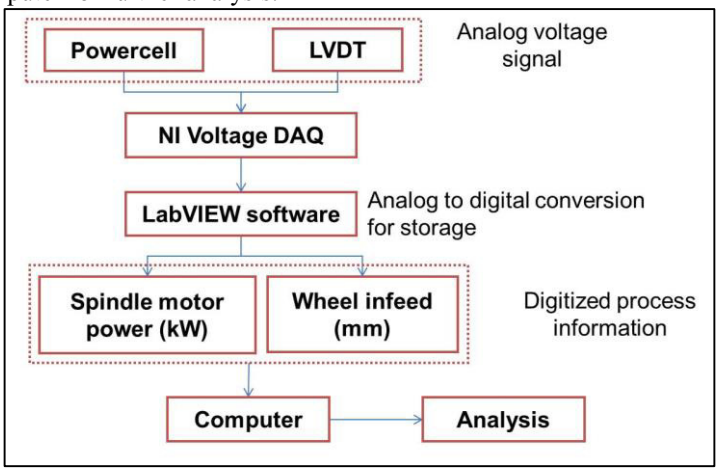

Figure 4: Data acquisition system and flow of information

Figure 5 shows the signal captured using powercell and LVDT during grinding of several components continuously without a dressing cycle. This signal represents the signature of this particular grinding process (Wei Tian, 2009). Figure 6 shows a schematic representation of a cylindrical grinding process with three stages i.e. roughing, finishing and spark-out.

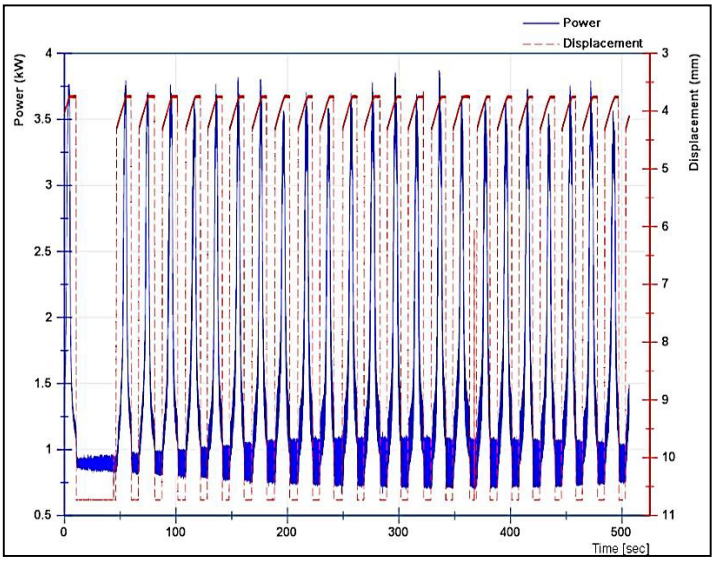

Figure 5: Grinding power and wheel infeed signals captured by data acquisition system for several grinding cycles

In Figure 6(a), the LVDT signal corresponding to the wheel infeed / plunging operation and the time taken for each stage in a grinding cycle is shown. The varying slope of the line indicates the varying feed rate applied to each stage of grinding and with no infeed for spark-out. Figure 6(b) shows the super-imposed power and infeed signal. Both power and infeed signals measurements are synchronized with time. Thus, as indicated in Figure 6(b), both signals can be superimposed to study the behaviour of grinding process with time. Representation of a grinding process by power and infeed signal is explained with a typical grinding cycle in the subsequent section.

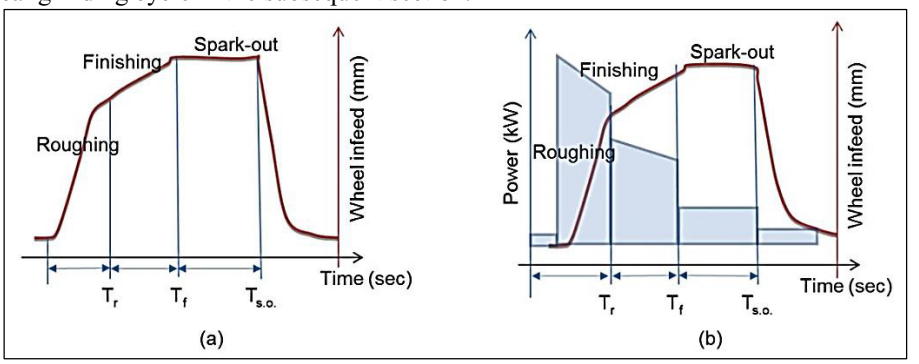

Figure 6: Schematic representation (a) Wheel infeed (LVDT signal) (b) Power and wheel infeed super-imposed

2.5 Mapping of different stages of grinding cycle with power and displacement signal

Figure 7 shows the variation of power and infeed of grinding wheel measured during different stages of grinding i.e. roughing, semi-finishing, finishing and spark-out, in a typical grinding cycle chosen for plunge grinding of a component i.e. grinding cycle of a component and are numbered as 3, 4, 5, and 6. From the variation of power in different stages of grinding, it is evident that the power drawn by spindle motor during roughing stage is higher due to higher rate as well as the magnitude of infeed of wheel into work. In contrast to this, semi-finishing and finishing stages employing smaller magnitude of infeed

with reduced infeed rate resulted in lower power, as shown in Figure 7. During spark-out, the power drawn by motor is very less and in most cases, it is slightly above the power drawn during idle running of motor.

The data collected during the grinding of components can be utilized to evaluate the process stability over a time period. Any substantial change in the trends or variation of power in different stages of grinding cycle can aid in identifying the status of grinding wheel such as sharp, worn out or glazed and also aid in assessing effect of dressing conditions, changes in the coolant application, etc.

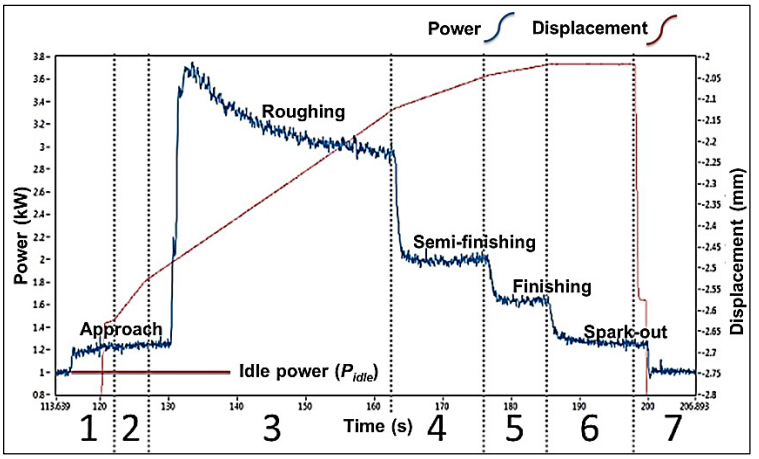

Figure 7: Different stages of grinding cycle represented by power and infeed measurement

2.6 Signal analysis and inferences

The variation of power in different stages of a grinding cycle over a period leads to direct inferences about the drift in grinding process behaviour. Figure 8 presents the power signal monitored over 'n' number of grinding cycles. During grinding, the topography of wheel undergoes changes due to wear of grit, fracture of bond and loading of chips into pores. All these phenomena increase the forces during grinding which in turn increase the power drawn by the spindle motor. Such a trend can be observed in the power signal monitored over cycle '1' to cycle 'n' (Wei Tian, 2009). Thus, this clearly suggests that a careful analysis of these plots can assess the status of grinding as well as grinding wheel.

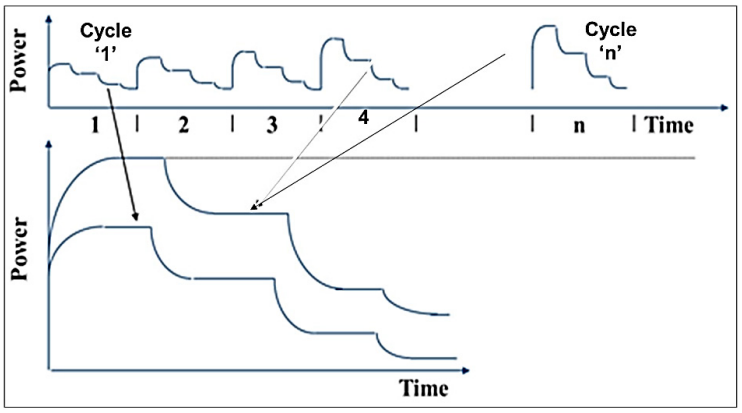

Figure 8: Increasing trend in power during continuous grinding without dressing

2.7 Estimation of MRR and specific cutting energy from infeed and power signal

A direct observation of the trends shown by the measured power signal gives an indication about the status of grinding process. In addition, the material removal rate (MRR), during each stage of grinding cycle, can be estimated from the grinding wheel infeed measured using LVDT. Both power and MRR can be used to derive certain basic parameters of grinding process like specific grinding energy and specific cutting energy. These quantities provide a better insight in to the grinding process with which the efficiency of the grinding process can be improved further.

Specific grinding energy is the total energy required per unit volume of material removed. It includes all the energy expended during a grinding process like specific energy for cutting (U_c), sliding/frictional energy and ploughing. Among these parameters, the specific cutting energy reflects the variation in grinding conditions in line with varying grinding power and monitoring this specific cutting energy leads to better control of the performance of grinding process. Figure 9 shows the determination of specific cutting energy from the power measured and MRR estimated. The MRR for a grinding cycle is estimated from work velocity (V_w), depth of cut (a_e) and grinding width (b_w). The displacement measured with LVDT is used to calculate the work velocity / infeed rate. This variation of MRR along with power can be used to derive the Specific cutting energy during grinding of a component (Subramanian 1992, Malkin and Guo 2008).

$$U_c = [(P_c)/Q_w] \qquad (1)$$

where P_c is the cutting power required for material removal during grinding. Powercell measures the absolute value of power that includes idle running power of spindle motor (P_{idle}) and grinding power (P) required for grinding of components through various stages of grinding cycle. This grinding power is given by the relation,

$$P = P_{th} + P_c \qquad (2)$$

where P_{th} – Threshold power, i.e. the power required to initiate the grinding process. This threshold power is highly influenced by the dressing conditions and grain type effects. The effect of friction due to abrasive grain sliding and the rubbing of bond against the work material, results in the threshold power (P_{th}). The influence of P_{th} decreases as MRR increases and thus results in lower specific energy in grinding at higher MRR. Figure 9 (a – d) shows the schematic representation of grinding cycles and the determination of specific cutting energy from measured power and MRR. Figure 9(a) shows the power measured during grinding cycle 1 immediately after dressing. Figure 9(b) shows the MRR for various stages of the grinding cycle plotted against the corresponding power. A straight line fit for the data shows several basic parameters like P_{th}, Pc and U_c. Figure 9(c) shows the power representation for 'n'th grinding cycle ground without any intermediate dressing. The same process parameters are maintained throughout 'n' cycles. From the figure, it is observed that the power drawn during different stages of grinding has increased. This can be attributed to the dulling of wheel due to continuous grinding without intermittent dressing as discussed in the section 2.6. Figure 9 (d) shows the variation of MRR in different stages of grinding cycle 'n' along with the corresponding power values. A straight line fit for this particular data is also presented in Figure 9(d). From the figure, it is observed that the specific cutting energy has increased from cycle '1' to cycle 'n' due to an increase in power, even though the MRR remained the same for all the stages. The difference in the cutting power P_c of cycle 'n' and cycle '1' referred to as P_f in Figure 9(d) reveals about the condition of the grinding process precisely. The power P_f depends on several factors like coolant flow, work material type and monitoring P_f will assist in controlling the process outcomes (Subramanian, 1999, 2015).

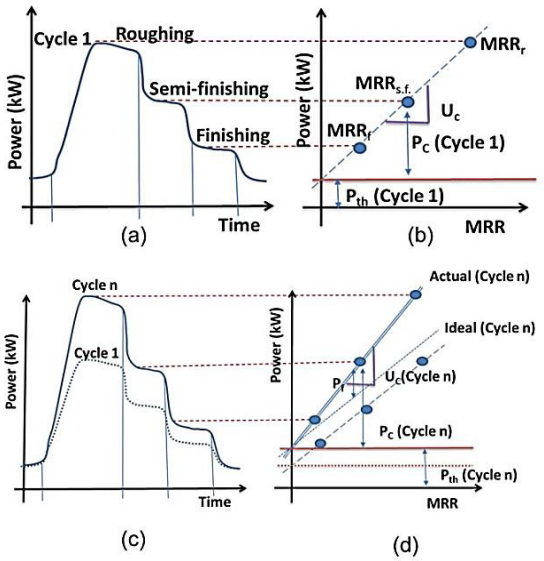

Figure 9: Determination of specific cutting energy from power and MRR
(a) Power signal of a grinding cycle 1 (b) MRR Vs Power for cycle 1
(c) Power signal of a grinding cycle 1 and 'n' super imposed
(d) MRR Vs Power for cycle 1 and cycle 'n' super imposed

3 Monitoring and analysis of grinding process using the diagnostic system

To demonstrate the application of diagnostic tool for assessing and improving the performance of grinding process, two different case studies were considered.

Case Study 1: Effect of dressing conditions on the performance of grinding process

Case Study 2: Estimation of dressing frequency using a diagnostic tool

3.1 Effect of dressing conditions on the performance of grinding process

The effectiveness of diagnostic tool in assessing the performance of grinding process is demonstrated by means of experimental trials in cylindrical grinding. Table 1 presents the details of machine, grinding wheel, dresser and conditions of grinding employed for the experiments. A hollow cylindrical component, mounted on a mandrel was held in between the centers during grinding.

Table 1: Process settings used in plunge grinding

Machine Tool	**Angular wheelhead CNC**
Work-material	D2 steel (60 HRC)
Wheel spec	A 80 J 5 V
Dresser spec	Blade type
Coolant type	Emulsion type (4%)
Operation	Cylindrical plunge grinding
Wheel speed	45 m/s
Work speed	26 m/min
Grinding length	10 mm

Table 2: Dressing condition

Case	Infeed (on dia) (mm)	Dressing overlap ratio	Passes
Fine	0.015	12	2
Coarse	0.040	6	2

Table 3: Grinding cycle details

Step	Stock removal (on dia) (mm)	Infeed rate (radial) (mm/min)	Material removal Rate MRR (mm^3/s)
Roughing	0.80	0.66	40.0
Semi-finishing	0.15	0.33	20.0
Finishing	0.05	0.16	10.0
Spark-out	15 revolutions		

Experimental trials considered the wheel dressed with two different dressing conditions, shown in Table **2**, but employed the same grinding cycle, shown in Table 3, for grinding of components of the same geometry. This particular choice is made since the dressing conditions change the topography on wheel surface and thus affects the performance of wheel in grinding. By monitoring the power and wheel infeed with diagnostic tool, the specific energy in grinding, using the wheel dressed by fine and coarse dressing can be determined.

Figure 10 shows the variation of power in different stages of grinding cycle employed while grinding of components with the wheel dressed by fine and coarse dressing. In both cases, the grinding cycle chosen for grinding of components is the same. This can be seen from the plot showing the same variation of infeed during the grinding cycle. The power drawn by the spindle motor in different stages of grinding cycle clearly shows that the power is higher in the grinding cycle with fine dressed wheel.

Figure 11 presents the variation of power with MRR in different stages of grinding. This clearly indicates the maximum power with large material removal rate during roughing stage. Using the data obtained with the diagnostic tool, the threshold power and specific energy in grinding are estimated, and are presented in Table 4. The threshold power (P_{th}) is the same for both dressing conditions, while the specific cutting energy (U_c) increased with decreasing material removal rate as the grinding progressed from roughing to finishing stage.

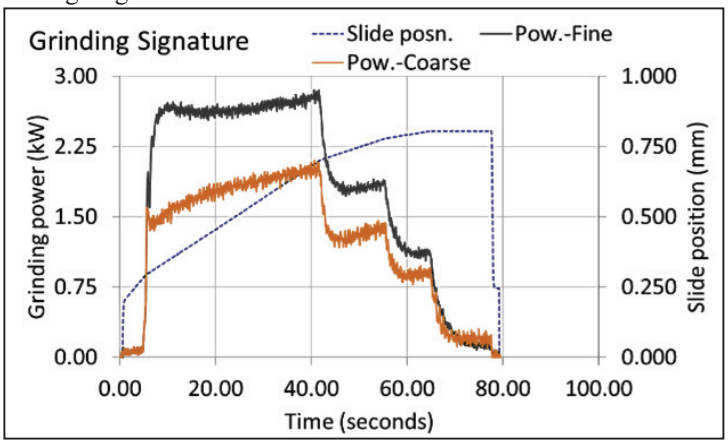

Figure 10: Variation of power during grinding cycle using wheel dressed with different dressing

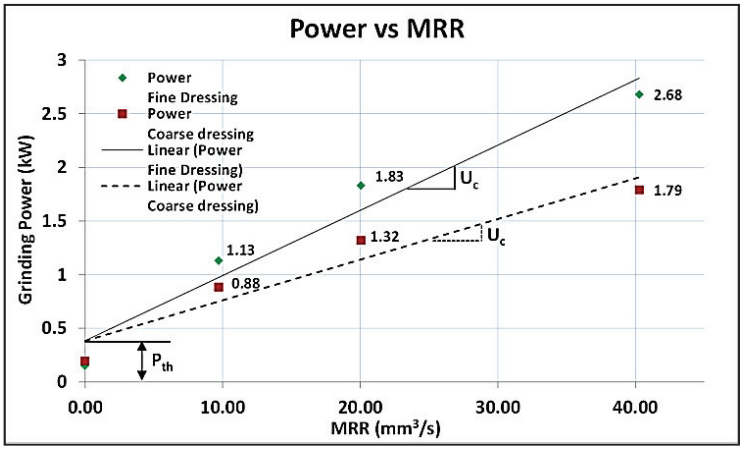

Figure 11: Variation of power with MRR during grinding using wheel dressed with different dressing conditions

Table 4: Derived Specific energy, threshold power and finish measured in grinding using fine and coarse dressed wheel

	Grinding cycle stage	MRR (mm^3/s)	Dressing condition	
			Fine	Coarse
Specific Grinding energy (U) (J/mm^3)	Roughing	40	69	50
	Semi-finishing	20	90	73
	Finishing	10	110	90
Specific cutting energy (U_c) (J/mm^3)			62	38
Threshold power (P_{th}) (W)			370	370
Surface Roughness (R_a)			0.32	0.56
Surface Roughness (R_z)			2.30	3.50

Figure 11 shows an increase in grinding power for finely dressed wheel. As discussed earlier, fine dressing conditions result in smooth surface on the wheel and thus results in higher chip friction during grinding. On the other hand, the rough surface produced by coarse grinding results in lesser grinding power. In addition, the specific cutting energy U_c during grinding with fine dressed wheel is higher compared to coarse dressed wheel. The higher U_c may be due to lesser chip space formed due to fine dressing conditions, resulting in more chip friction.

To confirm the nature of surface produced on the ground component by the wheel dressed with different conditions of dressing, the surface finish on the ground component is measured with a stylus type roughness measuring instrument and the results are shown in Table 4. From these results, it is observed that the wheel with finer dressing produced a smooth surface in contrast to a rough surface by coarse dressed wheel. Thus, the fine dressing of wheel results in a closed wheel surface morphology, which led to higher specific cutting energy (U_c) together with fine surface finish after grinding with the wheel, as clearly evident from the results.

The specific cutting energy depends on the equivalent chip thickness (h_{eq}), analogous with any machining process. Thus, U_c depends on the depth of cut during grinding. In grinding, the thickness of chip can be controlled by varying grinding process parameters or by changing the wheel characteristics with varying dressing conditions. With fine dressing condition i.e. less dressing depth and low dressing traverse rate, the wheel surface is less damaged resulting in fine topography on wheel surface. Such surface on wheel can lead to less chip space and can result in more chip friction, though the chip size remains the same. This is reflected in increased grinding power drawn by spindle motor. With coarse dressing condition, severe bond rupture occurs resulting in rougher wheel surface and better abrasive grit protrusion. This produces larger chip space and hence results in less chip friction. However, such a

wheel surface generates poor finish with lower specific grinding energy (Subramanian, 1995, 2015; Davis, 1974; Vairamuthu 2014).

Therefore, the measurement of power and infeed of wheel can aid one to assess the condition of wheel from time to time and the choice of suitable conditions for dressing to generate the desired topography on wheel surface.

3.2 Comparative study of performance of two different machines employing similar process setup

This case study illustrates the application of diagnostic tool to evaluate the utilization of two different machines employing the same grinding cycle for grinding a component with a view to change the periodicity of dressing in realizing the outcomes of grinding process.

Figure 12 shows the component that is ground in both machine A and machine B. Table 5, Table 6 and Table 7 list out the details of process and its set up, quality requirements, and wheel-work. The grinding cycle is monitored with the diagnostic tool in order to analyse the grinding process performance on both machines. The data collected from both machines were analysed to determine the following.

Diagnose grinding burn problem in machine B

Estimate the dressing frequency, i.e. the number of components that can be ground between successive dressings of grinding wheel in machine A

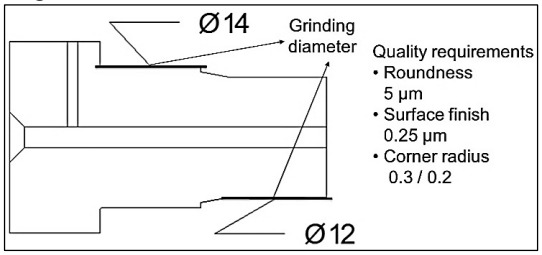

Figure 12: Part ground on cylindrical grinding machine

Table 5: Cylindrical grinding machine specifications – comparison chart

Machine	A	B
Model	Angular wheelhead CNC	Angular wheelhead hydraulic
Motor rating (kW)	5.5	3.75
Coolant Type and concentration (%)	Water soluble 3-4	Water soluble 4
Coolant pressure (bar)	2	1.5
Coolant flow (lpm)	120	80
Dresser	Blade type	Blade type

Table 6: Process setup details

Process parameter	Machine A	Machine B
Wheel Speed (rpm) / (mps)	1400 (42)	1400 (42)
Work Speed (rpm)	500	450
Dressing depth (µm)/ No of passes	80/ 2	65/ 2
Dressing traverse rate (mm/min)	80	60
Dressing skip (No of components)	40	60

Table 7: Details of wheel and work material

Grinding wheel	
Specification	A100L8VH
Design	Angular face (30°)
Size, shape, features	OD 600 x width 35 x ID 305 (all in mm)
Work Material	
Type / hardness	Ball bearing steel 60±2 HRC
Incoming Part Quality	Grinding stock 0.4 mm on outer diameter

3.2.1 Comparison of grinding cycle between machine A and machine B to diagnose grinding burn problem

From Table 5, 6 and 7, it could be observed that both machine A and machine B have been operated with similar input process parameters for producing the components. But, the components ground on machine B have shown burn marks on the part. In order to analyse the reasons for this deviation in part quality, the diagnostic tool was used to monitor the variation of wheel infeed during the grinding cycle. Variation in power combined with MRR in these two machines differed due to nature of control being different in both the machines. Machine A is CNC controlled machine whereas the machine B is hydraulically controlled machine.

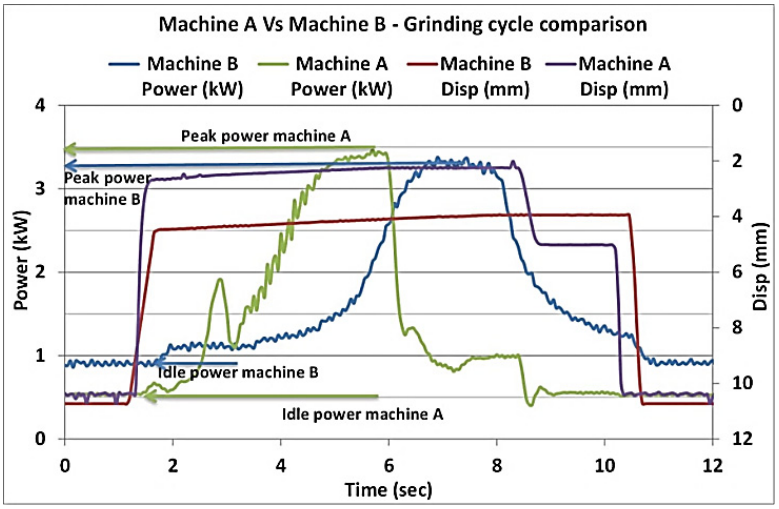

Figure 13: Grinding cycle comparison - Machine A vs Machine B

Figure 13 shows the variation of power and infeed with time for both machines A and B as explained in the section 2.5. The signals obtained from both these machines are superimposed in order to analyze the grinding cycle on a common time base.

From this figure, it can be seen that the cycle time is 9 seconds on machine A and machine B. The idle power and the peak power drawn by spindle motor of machine A is 0.5 kW and 3.5kW respectively, while the idle and peak powers on machine B are found to be 0.95 kW and 3.3 kW. Hence, it is important to get an insight into the process by analyzing the role of events between approach and retraction of wheel during plunge grinding. Figure 14 presents the breakup of the grinding process cycle starting from approach of the wheel for grinding to retraction of the wheel after grinding.

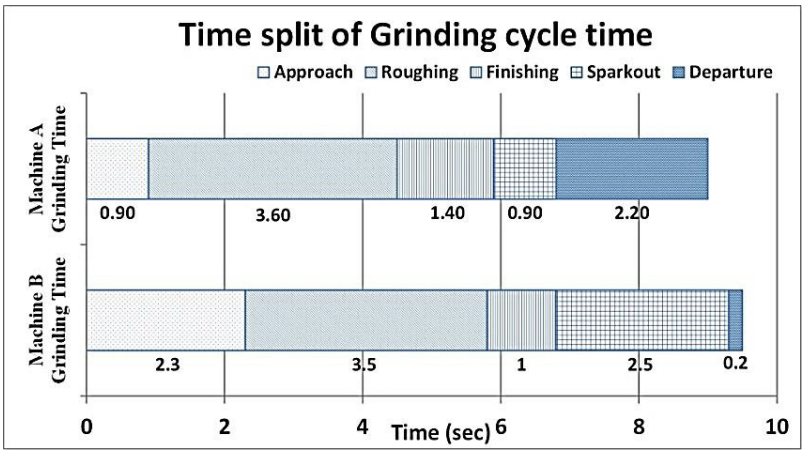

Figure 14: Time taken for different activities including approach and retraction of grinding wheel during a plunge grinding cycle

From this figure, it can be observed that the spark out time in machine B is about to 2.5 second while in machine A, it is 0.9 seconds. An excessive spark-out time combined with lower flow rate of coolant in machine B resulted in grinding burn on the surface of ground component. Further, the wheelhead slide in machine B is hydraulically controlled which has resulted in inconsistent control of infeed during different stages of grinding cycle.

By measuring the displacement of wheel slide with LVDT, the infeed rate of wheel could be made precisely along with the control of spark-out time and coolant flow rates similar to the conditions applied on machine A that avoided the thermal damage of ground component. Thus, the application of diagnostic system helped to monitor the process and aided in redesigning the grinding cycle of machine B in line with the one chosen with machine A.

3.2.2 Determination of frequency of dressing based on study of variation of peak power against time

From Table 6, it could be observed that the dressing skip of machine A is lesser than machine B, while both machines produce similar component with identical input process conditions. Dressing frequency is the number of components ground between two successive dressing cycles. Determination of dressing frequency plays a vital role in controlling the quality of ground component and enhancing the life of grinding wheel (Xiao, Malkin, Danai, 1992). Frequent dressings result in faster rate of wheel wear, while inadequate dressings can deteriorate the quality of ground components. Thus, a trade-off has to be established in arriving at the correct frequency of dressing. Moreover, this can also increase the use of grinding wheel. In general, the frequency of dressing is determined by a skilled operator with visual observation of surface quality on ground part, noise generated. However, with the help of diagnostic tool, it is possible to monitor the variation of process dynamics during grinding under varying conditions of wheel topography. This will also enable to decide about the correct dressing frequency with the chosen condition of dressing.

Figure 15 and Figure 16 shows the variation of peak power with grinding time while grinding a number of components after wheel dressing on machine B and machine A. From Figure 15, it can be observed that 40 components are ground between two dressing cycles on machine A. The peak power drawn for grinding the 40th component is found to be 3.36 kW.

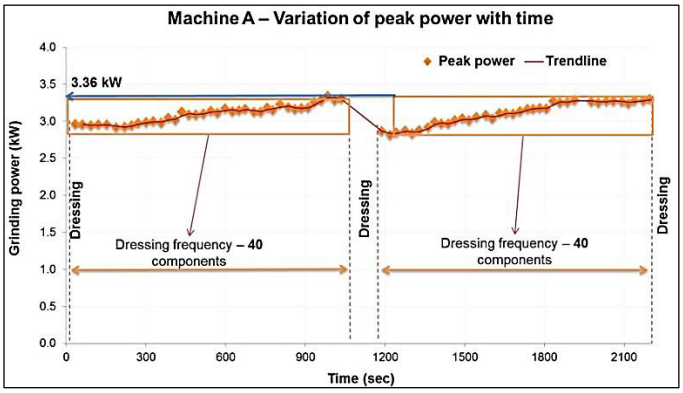

Figure 15: Variation of peak power with time – machine A for 40 jobs cycle

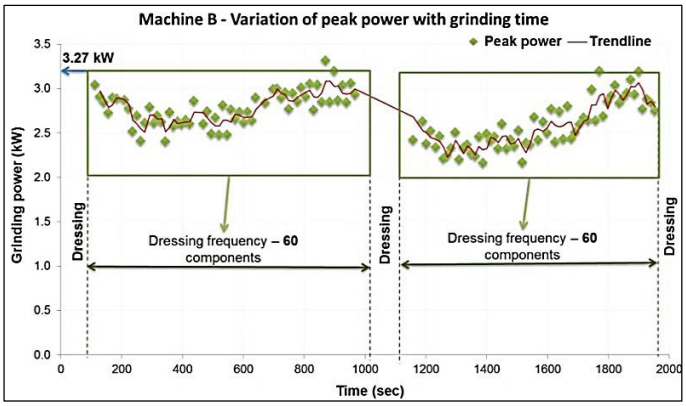

Figure 16: Variation of peak power with time – machine B

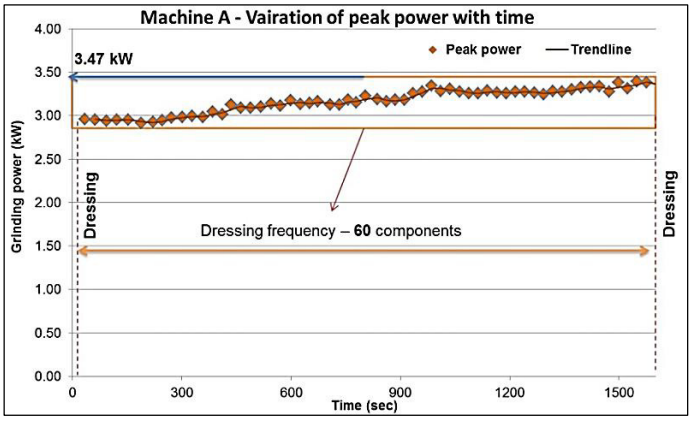

Figure 17: Variation of peak power with time – machine A for 60 jobs cycle

From Figure 16, it can be observed that 60 components were ground before dressing on machine B. The peak power drawn for grinding the 60th component is found to be 3.27 kW. From Table 5, it is evident that the wheel spindle motor capacity of machine A is 5.5 kW, while machine B has a spindle motor capacity of 3.75 kW. Thus, it is understood that maintaining a dressing frequency of 40 components results in underutilization of spindle motor capability of machine A, limiting its utility to 70% of its capacity. In order to enhance the utilization of machine A, a trial run was carried out by

increasing the dressing frequency to 60 components with the continuous monitoring of the process using the diagnostic system. Figure 17 shows the variation of power against time for set of components ground on machine A. From the figure, it can be observed that the peak power drawn during grinding of the 60th component is found to be 3.47 kW.

Moreover, the surface finish was measured on the component ground just before dressing on machine A and machine B. The measured R_a values are tabulated in Table 8. From the table it is found that the surface roughness of the 60th component ground in machine A is 0.241 µm R_a, and this value is well within the quality requirement as mentioned in Figure 12. Thus the dressing skip of machine A was increased to 60 components as in machine B, resulting in the increase of tool life of machine A.

Table 8: Surface roughness measured on ground components

Component Serial number	Surface roughness (R_a µm)	
	Machine A	Machine B
40	0.235	0.219
60	0.241	0.238

Thus, the application of diagnostic system assists in comparing the performance of grinding cycle of two different machines. This enables one to redesign an inconsistent process by benchmarking with an established process with a scientific approach.

4 Conclusion and future work

The assessment of performance of a cylindrical grinding process by monitoring the power drawn by spindle motor and grinding wheel infeed is realized with the developed in-process diagnostic system. Enhancing the efficiency of a cylindrical grinding process using the diagnostic system is investigated experimentally. The portability and non-intrusive nature of the diagnostic tool enabled the application of the diagnostic system in different machines and assisted in enhancing the optimum utility of the machine's capability. Future efforts are focused on to upgrade this diagnostic system to enable it to predict the failure of ground components by analyzing the specific grinding energy determined from the measured power and infeed data, thus enabling the grinding process to have automated process intelligence. In addition, efforts are focused on multi-sensor fusion to the diagnostic system to extend its applicability to industrial conditions and other material removal processes.

5 Acknowledgement

The authors would like to express their sincere thanks to the Office of Principal Scientific Adviser to Government of India for providing the financial support to this research work. Technical discussions on condition monitoring of grinding process and microscopic interactions of grinding process variables with Dr. K. (Subbu) Subramanian, President, STIMS Institute, USA are sincerely acknowledged.

References

Brinksmeier E, Heinzel C and Meyer L. Development and application of a wheel based process monitoring system in grinding. *CIRP Annals - Manufacturing Technology* 2005; 54(1): 301–304.

Byrne G, Dornfeld D, Inasaki I, Ketteler G, König W and Teti R. Tool Condition Monitoring TCM — The Status of Research and Industrial Application. *CIRP Annals - Manufacturing Technology* 1995; 44(2): 541-567.

Couey JA, Marsh ER, Knapp BR and Vallance RR. Monitoring force in precision cylindrical grinding. *Precision Engineering* 2005; 29(3): 307-314.

Davis CE. The dependence of grinding wheel performance on dressing procedure. *International Journal of Machine Tool Design and Research* 1974; 14(1): 33-52.

Graham D and Webster JA. A practical, portable hardware/software system monitors and records creepfeed grindings "vital signs" to minimize thermal damage System takes grindings temperature. *American machinist* Dec 2003.

Inasaki I and Okamura K. Monitoring of Dressing and Grinding Processes with Acoustic Emission Signals. *CIRP Annals - Manufacturing Technology* 1985; 34(1): 277-280.

Inasaki I. Sensor Fusion for Monitoring and Controlling Grinding Processes. *The International journal of advanced manufacturing technology* 1999; 15(10): 730-736.

Jardine AKS, Lin D and Banjevic D. A review on machinery diagnostics and prognostics implementing condition-based maintenance. *Mechanical Systems and Signal Processing* 2006; 20(7): 1483-1510.

Karpuschewski B, Wehmeier M and Inasaki I. Grinding monitoring system based on power and acoustic emission sensors. *CIRP Annals - Manufacturing Technology* 2000; 49(1): 235-240.

Karpuschewski B and Inasaki I. *Chapter 3 - Monitoring systems for grinding process,* Condition Monitoring and Control for Intelligent Manufacturing, London: Springer, pp.83-107, 2006, ISBN: 978-1-84628-268-3.

Malkin S and Guo C. *Chapter 5 - Grinding mechanisms.* Grinding technology: theory and application of machining with abrasives, (2nd Ed.), New York: Industrial press, pp.115-156, 2008, ISBN: 978-0-83113-247-7.

Oliveira JFG, Silva EJ, Guo C and Hashimoto F. Industrial challenges in grinding. *CIRP Annals - Manufacturing Technology* 2009; 58(2): 663-680.

Pawel L, Jan Rafalowicz and Jerzy J. An Intelligent Monitoring System for Cylindrical Grinding. *CIRP Annals - Manufacturing Technology* 1993; 42(1): 393-396.

Subramanian K and Lindsay RP. A Systems Approach for the Use of Vitrified Bonded Superabrasive Wheels for Precision Production Grinding. *ASME Transactions, Journal of Engineering for Industry* 1992; 114(1): 41-52.

Subramanian K. *Finishing Methods Using Multiple or Random cutting Edges Section*. Surface Engineering, Volume 5, ASM Handbook, ASM International, pp.90-109, 1994, ISBN: 978-0-87170-384-2.

Subramanian K. Measurement and Analysis of Grinding Processes. *Abrasives Magazine*, April - May. 1999.

Subramanian K, Ananat Jain, Vairamuthu R and Brij M Bhushan. Tribology as an Enabler for Innovation in Surface Generation Processes. In: *Proc. of the IMECE'15,* 2015, pp.1-11.

Tönshoff HK, Friemuth T and Becker JC. Process Monitoring in Grinding. *CIRP Annals - Manufacturing Technology* 2002; 51(2): 551-557.

Vairamuthu R, Brij M Bhushan, Srikanth R and Ramesh Babu N. Performance Analysis of Cylindrical Grinding Process with a Portable Diagnostic Tool. In: *Proc. of the AIMTDR'14,* 2014, pp.1-6, 582.

Wei Tian. *Signature analysis of OD grinding processes with applications in monitoring and diagnosis*. MS thesis, 2009; Worcester Polytechnic Institute, Worcester, Massachusetts, USA.

Xiao G, Malkin S and Danai K. Intelligent Control of Cylindrical Plunge grinding. In: *Proc of the ACC'92*, 1992, pp.391-399.